



# Cold Spring Harbor Protocols

## Optically Induced Occlusion of Single Blood Vessels in Rodent Neocortex

Andy Y. Shih, Nozomi Nishimura, John Nguyen, Beth Friedman, Patrick D. Lyden, Chris B. Schaffer and David Kleinfeld

*Cold Spring Harb Protoc*; doi: 10.1101/pdb.prot079509

---

### Email Alerting Service

Receive free email alerts when new articles cite this article - [click here](#).

---

### Subject Categories

Browse articles on similar topics from *Cold Spring Harbor Protocols*.

[Fluorescence](#) (394 articles)  
[Fluorescence, general](#) (265 articles)  
[Imaging for Neuroscience](#) (254 articles)  
[Mouse](#) (270 articles)  
[Multi-Photon Microscopy](#) (78 articles)  
[Neuroscience, general](#) (234 articles)

---

To subscribe to *Cold Spring Harbor Protocols* go to:  
<http://cshprotocols.cshlp.org/subscriptions>

## Protocol

# Optically Induced Occlusion of Single Blood Vessels in Rodent Neocortex

Andy Y. Shih, Nozomi Nishimura, John Nguyen, Beth Friedman, Patrick D. Lyden, Chris B. Schaffer, and David Kleinfeld

The ability to form targeted vascular occlusions in small vessels of the brain is an important technique for studying the microscopic basis of cerebral ischemia. We describe two complementary methods that enable targeted occlusion of any single blood vessel within the upper 500  $\mu\text{m}$  of adult rodent neocortex. Our goal is to generate highly localized regions of ischemia by blocking penetrating arterioles and ascending venules, which are bottlenecks of flow in the cortical angioarchitecture. One method, termed photothrombosis, makes use of linear optical absorption by a photosensitizer, transiently circulated in the blood stream, to induce a clot in a surface or near-surface segment of a vessel. The second method, termed plasma-mediated ablation, makes use of nonlinear optical interactions, without the need to introduce an exogenous absorber, to induce clots in subsurface segments of penetrating vessels, as well as subsurface microvessels and capillaries. The choice of the method for occlusion of individual vessels depends on the location of the vessels being studied and the objectives of the study. Here we describe concurrent high resolution in vivo imaging and auxiliary laser setups, occlusion protocols, and post hoc histological procedures.

## MATERIALS

It is essential that you consult the appropriate Material Safety Data Sheets and your institution's Environmental Health and Safety Office for proper handling of equipment and hazardous material used in this protocol.

### Reagents

Agarose

Fluorescein-dextran (2 MDa; 5% [w/v] in saline) (Sigma-Aldrich)

*Texas Red-dextran (70 kDa) (Life Technologies) can also be used as a fluorescent probe.*

Rose Bengal (1% [w/v] in saline; filtered before use)

Sucrose (30%, w/v)

### Equipment

Amplified Ti:sapphire 100-fsec laser source (Libra from Coherent, Inc.)

Brain matrix (RSMAC-2 from Plastics One, Inc.)

Continuous-wave 530-nm laser source (Edmund Optics)

Fine tungsten electrodes

Glass slides

Imaging software (Nguyen et al. 2006, 2009)

Adapted from *Imaging in Neuroscience* (ed. Helmchen and Konnerth). CSHL Press, Cold Spring Harbor, NY, USA, 2011.

© 2013 Cold Spring Harbor Laboratory Press

Cite this protocol as *Cold Spring Harb Protoc*; 2013; doi:10.1101/pdb.prot079509

### Objective lenses

For low magnification, use a 4×, 0.28 NA objective (UB950; Olympus) or a 10×, 0.3 NA objective (W Achroplan; Zeiss). For high resolution, use a 40×, 0.8 NA objective (UM568; Olympus).

### Two-photon laser-scanning microscope

We integrate additional lasers into a custom-built two-photon imaging system for photothrombosis and plasma-mediated ablation (Fig. 1A; Majewska et al. 2000; Tsai and Kleinfeld 2009). Additionally, Sigler et al. (2008) have described methods to convert an Olympus BX series microscope for photothrombosis of single vessels. These and other schemes that combine imaging and ablation beams before the scan mirrors may be adapted for a commercial instrument, the Ultima Multiphoton Microscopy System with an optional high-speed two-photon optics set and external detector (Prairie Technologies).

## METHOD

### 1. Prepare a cranial imaging window in an experimental rodent of choice.

Detailed procedures for animal preparation and the generation of a cranial imaging window in the rat are presented in Kleinfeld and Delaney (1996), Kleinfeld and Denk (2000), and Kleinfeld et al. (2008). The approaches described in this protocol can also be applied to mice, and details of mouse cranial window preparations can be found in Xu et al. (2007), Holtmaat et al. (2009), and Drew et al. (2010).

### Photothrombotic Occlusion

Targeted photothrombosis can be used to occlude individual arterioles and venules that lie on or near the cortical surface.

### 2. Inject a 1.0 mL/kg bolus of 5% fluorescein–dextran solution in saline into either a femoral vein catheter or directly into a tail vein.

Labeling the blood plasma with 2-MDa fluorescein–dextran provides contrast between the red blood cells (RBCs) and the plasma (Kleinfeld et al. 1998). The high-molecular-weight dextran provides stable labeling, typically for at least 3 h. Supplement the dye at 0.3 mL/kg, as needed during imaging.

### 3. Obtain a three-dimensional stack of images of the cerebral vessels throughout the cranial window to use as a navigational map (Fig. 1B). Start at low magnification, typically with a 4×, 0.28 NA objective or a 10×, 0.3 NA objective.

Higher resolution imaging of local vascular architecture and vasodynamics, such as RBC speed and vessel diameter (Shih et al. 2009), are typically obtained with a 40×, 0.8 NA objective.

### 4. Select a penetrating arteriole or ascending venule to target for occlusion (Fig. 1C). Targeting vessels that have a segment coursing parallel to the cortical surface allows for easy verification of clot formation.

Note that cortical arterioles appear smoother and straighter than venules and have fewer branching points. The location of penetrating arterioles and ascending venules can be identified by manually tracing through the pial arterial and venous networks (Fig. 1B). Arterioles and venules can also be differentiated based on direction of flow (i.e., into or out of the cortex).

### 5. Inject a 1.0 mL/kg bolus of 1% (w/v) Rose Bengal solution in saline through the femoral vein catheter or tail vein.

Rose Bengal should be injected immediately before forming the occlusion, since it is cleared from the blood stream within minutes (Zhang et al. 2005).

### 6. Initiate photothrombosis by aiming the focal point of the green laser within the lumen of the target vessel, near the vessel wall (Fig. 1D). This will nucleate the clotting cascade and create an attachment point for the growing clot. If a clot does not occur within 5–10 sec of irradiation, inject a 0.5 mL/kg supplement of Rose Bengal solution.

A 50-mW green laser light (Edmund Optics) is introduced into the imaging beam path with dichroic mirror 1 (625 DRLP, Chroma) (Fig. 1A). The focal point of the beam is fixed, centered along the optical axis, and controlled by a shutter (LS3Z2 Uniblitz and VMM-D1 driver, Vincent). The beam is adjusted to pass through a 3.5-mm-diameter clearing that was etched in the dielectric coating of dichroic mirror 2 (700 DCXRU, Chroma) (Fig. 1A). This allows transmission of the green laser while still reflecting >90% of emitted light from the sample toward the PMTs. As the interval of irradiation is typically long (i.e., 50–100 sec), irradiation

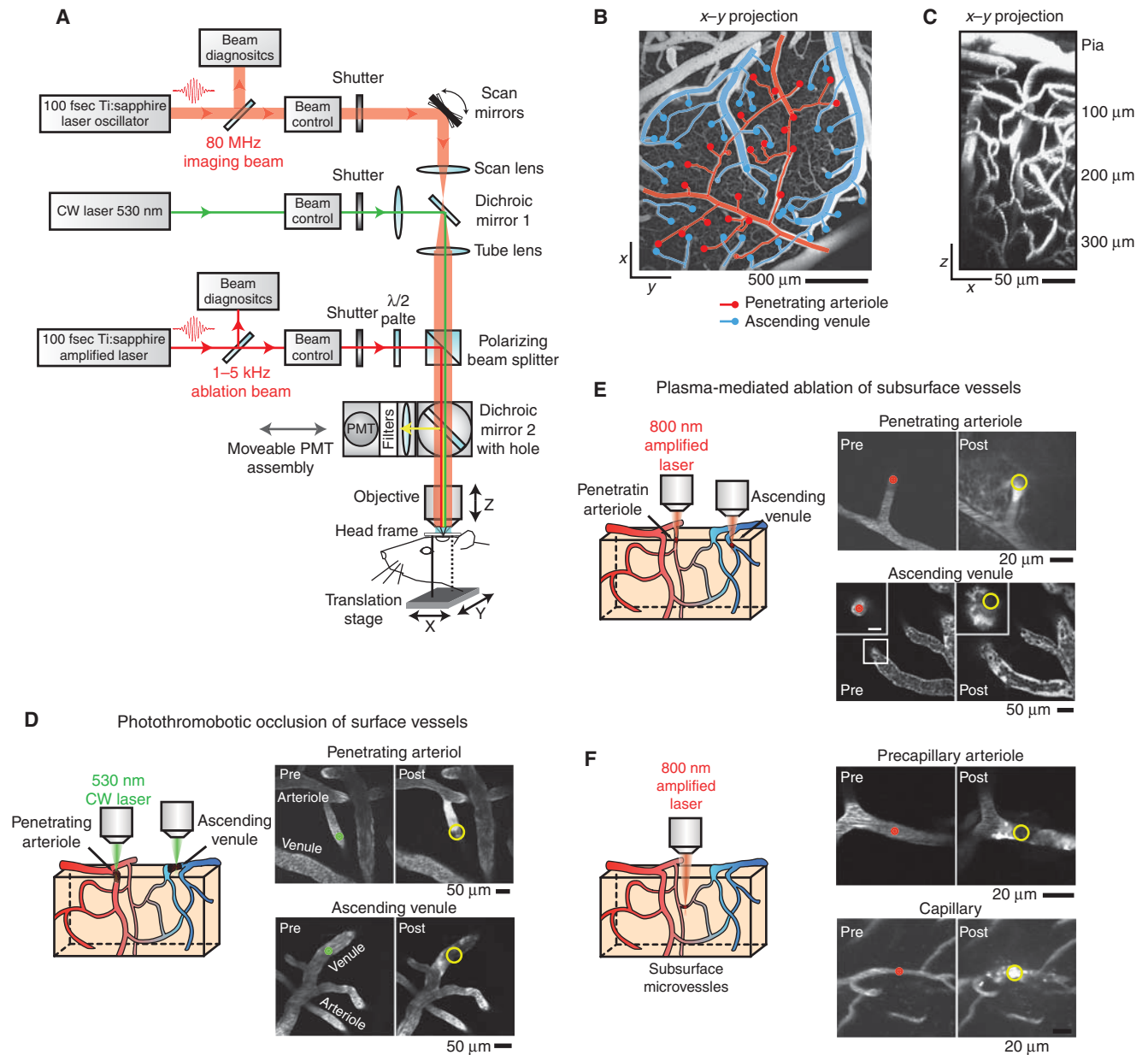


**FIGURE 1.** Forming intravascular occlusions in single cortical vessels using photothrombosis or plasma-mediated ablation. (A) Schematic of a two-photon laser-scanning microscope (TPLSM) system modified to include a continuous-wave green-light laser for photothrombosis and an amplified pulsed laser for plasma-mediated ablation. (CW) Continuous wave; (PMT) photomultiplier tube. The beam control module refers to a device for control of laser intensity, a pair of lenses for beam shaping, and a prism pair for pulse dispersion compensation, if required. (B) x-y maximal projection of a TPLSM image stack showing pial vessels and fine microvessels through a rat cranial window. A manual tracing of arteriole (red) and venule (blue) networks is overlaid on the image. The locations of penetrating arterioles and ascending venules are marked with circles. (C) x-z maximal projection of TPLSM image stack showing a single penetrating arteriole, typical of those selected for targeted occlusion. (D) (Left) Schematic of vessel types that can be targeted by focused photothrombosis (i.e., penetrating arterioles and ascending venules). (Right) Examples of pre- and postocclusion images from rat. (E-F) Schematic of vessel types that can be targeted by plasma-mediated ablation (i.e., penetrating arterioles, ascending venules, or deep microvessels). Pre- and postocclusion examples for each vessel class are shown. The inset within the ascending venule example shows a subsurface imaging plane 100  $\mu\text{m}$  deep where the clot was formed. The capillary image in (F) was obtained from an Alzheimer's mouse model. All other example images are from adult rat.

is periodically interrupted for brief epochs of imaging, typically 1 frame (0.2 sec per frame) every 1 sec for an 80% duty cycle. This permits formation of the clot to be observed in real time. Alternatively, the PMT assembly can be temporarily moved out of the path to allow the green laser light to pass. However, observation of the formation of the clot is recommended to avoid excessive irradiation and unintended photothrombosis in neighboring vessels. The green laser is brought to the same focal plane as the imaging beam of the two-photon microscope using an appropriate telescope and centered in the imaging field. When using a 40 $\times$ , 0.8 NA dipping objective with an underfilled back aperture, the final green laser spot size is  $\sim 3\ \mu\text{m}$  in diameter. In all cases, the intensity of the laser light at the focus should initially be adjusted to  $\sim 1\ \text{mW}$  using a tunable neutral density filter and may be increased as needed. The motorized/encoding x–y stage of the microscope is used to reposition the animal to change the location of photoactivation (Fig. 1A). Alternatively, additional lasers may be introduced through a second set of scanners so that the position of irradiation may be shifted electromechanically (i.e., the Ultima with an optional second set of scanners).

7. Traverse the focus of the green laser across the diameter of the blood vessel to facilitate thrombus formation. Occlusion may require 10–100 sec of irradiation. Larger vessels with relatively fast RBC flow require more time to fully occlude; the exact time must be determined empirically. A successful occlusion appears densely packed with immobile nonfluorescent RBCs often surrounded by a brighter region of stagnant fluorescent plasma (Fig. 1D).
8. Collect postocclusion measurements, as desired.

## Plasma-Mediated Occlusion

Plasma-mediated ablation makes use of the dissociation of matter by high fluence, 100 to 300-fsec pulses of near-infrared light (Schaffer et al. 2001; Tsai et al. 2004, 2009). These pulses ionize the material, such as blood plasma or vascular endothelium, within a femtoliter-sized focal volume of the incident laser pulse. This method allows occlusions of microvessels and capillaries deep below the surface of the cortex, typically down to 500  $\mu\text{m}$ , but in principle down to 1000  $\mu\text{m}$  below the pia, without disruption of the neighboring tissue. Plasma-mediated ablation is also well suited for inducing clots in penetrating arterioles and ascending venules, by targeting subsurface segments of the vascular tree. However, this method is not suitable for targeting arterioles that lie on the cortical surface, which tend to hemorrhage and obscure subsequent imaging.

9. Collect baseline vascular image stacks. To resolve deep microvessels, this should be performed at high resolution using a 40 $\times$  objective.
10. Select a subsurface segment of vasculature for targeted occlusion. This could be penetrating arterioles, ascending venules, or subsurface microvessels.

### To occlude Penetrating Arterioles and Ascending Venules

11. Place the focus of the amplified beam about halfway between the brain surface and the first capillary branch off of the vessel (Fig. 1E). The laser focus should be located within the vessel lumen a few micrometers from the vessel wall.
12. Irradiate with one pulse using an energy that is below the expected damage threshold. This starting energy is depth dependent (i.e.,  $\sim 50\ \text{nJ}$  at 20  $\mu\text{m}$  depth and 150 nJ at 150  $\mu\text{m}$  depth).

An amplified 100-fsec light source is introduced into the beam path through a polarizing beam splitter (Fig. 1A). As with the case of green laser light, it may also be introduced in other locations along the path of the imaging beam. This beam is focused to the same plane as the imaging laser and aligned such that photodisruption occurs at the center of the imaged field. The energy per pulse of the photodisruption beam is coarsely varied with a tunable neutral density filter and finely varied with a  $\lambda/2$  plate followed by a polarizing beam splitter. The number of pulses is controlled by a fast shutter (LS3Z2 Uniblitz and VMM-D1 driver). The diameter of the amplified beam is adjusted with an appropriate telescope to overfill the back aperture of the objective. This is necessary to obtain the smallest possible spot size for the amplified beam, which is on the order of a femtoliter. The energy per pulse is initially set to 30 nJ at the focus of a 40 $\times$ , 0.8 NA dipping objective, which is near the threshold fluence for damage of  $\sim 1\ \text{J}/\text{cm}^2$ . For a 5-kHz, 100-fsec amplified laser, this corresponds to an average power of 0.15 mW.

13. Increase the number of pulses by factors of 10 with the same energy, often trying each pulse number a few times while watching for signs of laser damage. The first visual indication of photodisruption is extravasation of fluorescein–dextran outside the vessel lumen (Fig. 1E). If extravasation fails to occur, increase the pulse energy by  $\sim 25\%$  and repeat the procedure described above.

- Once extravasation occurs, repeat the irradiation with the threshold energy and number of pulses, while targeting multiple nearby areas along the inner wall of the vessel segment.
- Continue to irradiate the targeted segment until there is a complete cessation of RBC movement in the target vessel. To verify successful occlusion, return to the cortical surface and ensure that flow has ceased in the main branch of the arteriole or venule.

*Increasing the energy too high results in the rupture of the vessel and a large hemorrhage (Nishimura et al. 2006).*

### To Occlude Subsurface Microvessels

- Aim the focal point of the amplified beam into the vessel lumen, a few micrometers away from the vessel wall (Fig. 1F). Use a graded approach to irradiation similar to that described above. It is critical to identify a segment of the targeted vessel where RBC movement can be readily visualized to confirm successful occlusion.

## Histology

*It is often desirable to examine the consequences of single-vessel occlusion using post hoc histology. A number of strategies can be used to relocate the occluded vessel and the corresponding cyst in perfused tissue (Fig. 2A–C). A fluorescent vascular casting method can be used to visualize the pial vasculature during histological processing.*

- Inject a fluorescein–dextran–agarose mixture transcardially as described in Tsai et al. (2005) and Shih et al. (2009).

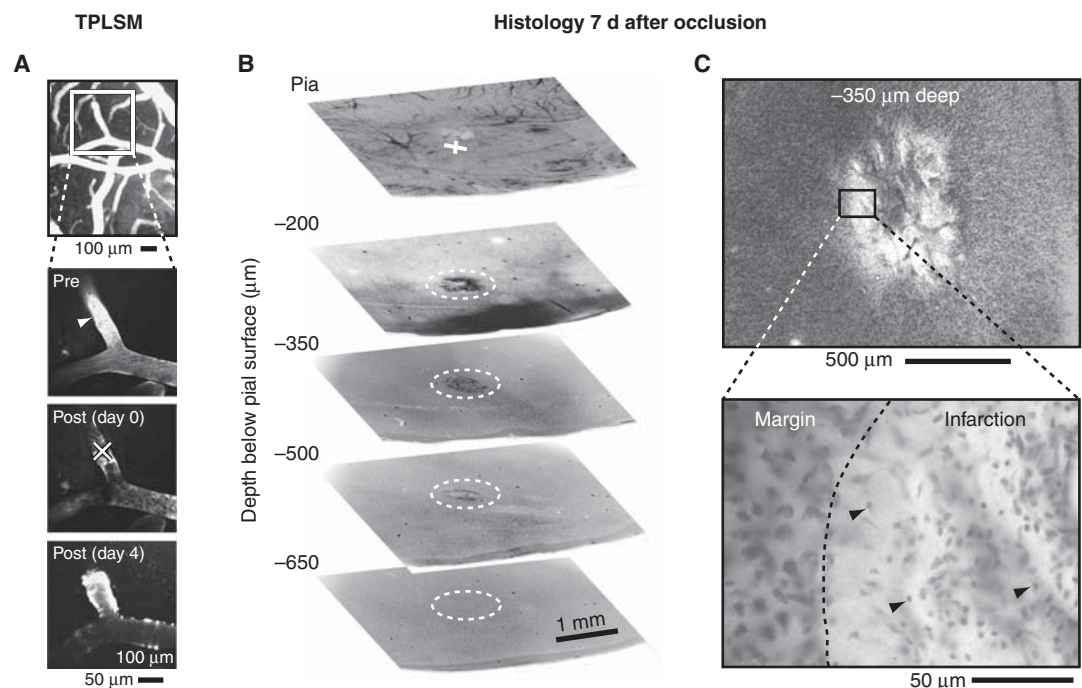


**FIGURE 2.** Photothrombotic occlusion of penetrating arterioles using Rose Bengal. (A)  $x - y$  maximal projected TPLSM image showing a single penetrating arteriole to be occluded by photothrombosis. (Inset images) The occluded vessel before and after occlusion. Note the extravasation of fluorescein–dextran dye from the vessel 4 d after stroke, which indicates damage to the vascular wall. (B) Examination of the cyst volume 7 d after occlusion in Cresyl Violet-stained tissue sections. The animal was perfused with a vascular cast, and the cortex was flattened. The occluded vessel, marked by an  $\times$  symbol, was located in the fixed tissue by using a fluorescent vascular cast as a map. The fluorescent vessels are visible at the pial surface. Electrolytic fiducials (not shown) were made through the thickness of the cortex at the time of perfusion, and fixation aided tissue re-alignment after serial sectioning. The image intensities were inverted for improved visualization. (C) Magnified view of Cresyl Violet-stained brain sections. Note the shrunken pyknotic cells that are widespread within the core of the microinfarction (black arrowheads).

18. Because this dye remains in situ after tissue fixation, use it to map the exact location of the targeted vessel, based on unique features in the pial vascular topology that are visible through the imaging window.
19. Excise the region of interest in a coronal orientation using a brain matrix.
20. Cryoprotect the blocked tissue in 30% sucrose overnight and further cryosection it for immunohistology.

*The microinfarction can also be viewed in a flattened cortex preparation that is cryosectioned tangentially to the cortical surface.*
21. View the microinfarction in a flattened cortex preparation after fluorescent casting of the vasculature (Fig. 2B). Excise the cortex, sandwich it between two glass slides separated by a distance of 2.5 mm, and postfix it overnight.
22. Locate the target vessel and then generate fiducial marks in its vicinity by applying current through fine tungsten electrodes that are advanced through the thickness of the cortex. This creates burn marks in each section that are used for alignment of serial tissue sections after cryosectioning tangentially to the cortical surface.

## DISCUSSION

Advances in imaging techniques, such as two-photon laser scanning microscopy, combined with various methods to label and record cellular activity in vivo, have greatly improved both spatial and temporal resolution for studying pathological processes in real time (Misgeld and Kerschensteiner 2006). These methods are important for the study of pathological mechanisms that underlie ischemic injury, including abnormal changes in cell signaling and structure, vascular dysfunction, and inflammation.

Here we consider two complementary approaches to selectively occlude single vessels anywhere within the upper 500  $\mu\text{m}$  of cerebral cortex. Photothrombosis uses linear optical absorption by a photosensitizer, transiently circulating in the blood stream, to initiate a clotting cascade in vessels on the cortical surface (Watson et al. 1985; Schaffer et al. 2006; Nishimura et al. 2007; Sigler et al. 2008). Plasma-mediated ablation makes use of nonlinear optical interactions, without the need to introduce an exogenous absorber, to induce clots in subsurface vessels and capillaries (Nishimura et al. 2006, 2010; Nguyen et al. 2007). Both techniques complement an existing variety of preclinical stroke models that generate larger areas of ischemia (Ginsberg and Busto 1989). The advantages of this targeted approach include the ability to (1) select a specific class of cortical vessel (i.e., capillary vs. surface arteriole or venule); (2) select a specific location for ischemia within the imaging window (i.e., a cortical column); (3) make pre- and postmeasurements of hemodynamic and neuronal state variables; and (4) initiate the ischemic event in situ under the microscope.

Our goal is to exploit the physical localization of highly focused laser light to form occlusions within “bottleneck” vessels of the cortical angioarchitecture. Occlusions of either penetrating arterioles (Nishimura et al. 2007) or ascending venules (Nguyen et al. 2007) have a large impact on cortical blood flow. Furthermore, the columnar regions of ischemia generated by such occlusion are capable of developing into cortical microinfarctions over several days.

## Example Application

Both of the techniques described here are appropriate for chronic as well as acute studies. An example longitudinal study shows that occlusion of even a single penetrating arteriole leads to discrete regions of cortical ischemia and tissue damage (Fig. 2B,C; see Blinder et al. 2010). The accuracy in this technique allows one to investigate the functional consequences of ischemia on cells neighboring the targeted vessel, by, for example, using mice with genetically labeled cell populations (Feng et al. 2000) or after loading tissue with organic  $\text{Ca}^{2+}$  dyes (Stosiek et al. 2003; Ding et al. 2009). Further-

more, these occlusions provide a means to model and study the consequences of vascular disease and small-scale strokes that occur in the aging human cortex (Suter et al. 2002; Kovari et al. 2004). Although the examples described here are from the rat, it is anticipated that future studies will take advantage of various genetically engineered mouse lines, which appear to be particularly amenable to longitudinal imaging after photothrombosis (Brown et al. 2007; Drew et al. 2010).

## Limitations

Two caveats of photothrombosis are noteworthy. First, small thrombi formed during the period of illumination may travel downstream rather than stick at the site of irradiation. It is difficult to track the location and stability of these unintentional thrombi, and thus their impact on blood flow is unknown. Second, even well-formed clots tend to dislodge or disintegrate over the long term, particularly in fast-flowing arterioles. Although most clots are stable for at least 5–6 h, over the course of a typical experiment, the exact timing of natural deocclusion can vary greatly from vessel to vessel. Thus, the effects of reperfusion injury would be difficult to assess in this model. However, future approaches may be able to improve control over recanalization by irradiating the clot with ultraviolet light (Watson et al. 2002). Lastly, one caveat of the plasma-mediated ablation method is that excessive damage to the vessel wall is likely to cause hemorrhaging.

## ACKNOWLEDGMENTS

We thank Jonathan D. Driscoll for critical reading of the manuscript. This work was funded by the National Institutes of Health (grants EB003832, MH085499, and NS059832 to D.K. and NS43300 and NS052565 to P.D.L.), the Ellison Medical Foundation (grant AG-NS-0330-06 to C.B.S.), the American Heart Association (grant 0735644T to C.B.S.), the VA Medical Research Foundation (grant to P. D.L.), and a postdoctoral fellowship from the American Heart Association to A.Y.S.

## REFERENCES

- Blinder P, Shih AY, Rafie C, Kleinfeld D. 2010. Topological basis for the robust distribution of blood to rodent neocortex. *Proc Natl Acad Sci* 107: 12670–12675.
- Brown CE, Li P, Boyd JD, Delaney KR, Murphy TH. 2007. Extensive turnover of dendritic spines and vascular remodeling in cortical tissues recovering from stroke. *J Neurosci* 27: 4101–4109.
- Ding S, Wang T, Cui W, Haydon PG. 2009. Photothrombosis ischemia stimulates a sustained astrocytic  $Ca^{2+}$  signaling in vivo. *Glia* 57: 767–776.
- Drew PJ, Shih AY, Driscoll JD, Knutsen PM, Blinder P, Davalos D, Akassoglou K, Tsai P, Kleinfeld D. 2010. Chronic optical access through a polished and reinforced thinned skull. *Nature Methods* 7: 981–984.
- Feng G, Mellor RH, Bernstein M, Keller-Peck C, Nguyen QT, Wallace M, Nerbonne JM, Lichtman JW, Sanes JR. 2000. Imaging neuronal subsets in transgenic mice expressing multiple spectral variants of GFP. *Neuron* 28: 41–51.
- Ginsberg MD, Busto R. 1989. Rodent models of cerebral ischemia. *Stroke* 20: 1627–1642.
- Holtmaat A, Bonhoeffer T, Chow DK, Chuckowree J, De Paola V, Hofer SB, Hübener M, Keck T, Knott G, Lee WC, et al. 2009. Long-term, high-resolution imaging in the mouse neocortex through a chronic cranial window. *Nat Protoc* 4: 1128–1144.
- Kleinfeld D, Delaney KR. 1996. Distributed representation of vibrissa movement in the upper layers of somatosensory cortex revealed with voltage sensitive dyes. *J Comp Neurol* 375: 89–108.
- Kleinfeld D, Denk W. 2000. Two-photon imaging of neocortical microcirculation. In *Imaging neurons: A laboratory manual* (ed. Yuste R, et al.), pp. 23.1–23.15. Cold Spring Harbor Laboratory Press, Cold Spring Harbor, NY.
- Kleinfeld D, Mitra PP, Helmchen F, Denk W. 1998. Fluctuations and stimulus-induced changes in blood flow observed in individual capillaries in layers 2 through 4 of rat neocortex. *Proc Natl Acad Sci* 95: 15741–15746.
- Kleinfeld D, Friedman B, Lyden PD, Shih AY. 2008. Targeted occlusion to surface and deep vessels in neocortex via linear and nonlinear optical absorption. In *Animal models of acute neurological injuries* (ed. Chen J, et al.), pp. 169–185. Humana Press, Totowa, NJ.
- Kovari E, Gold G, Herrmann FR, Canuto A, Hof PR, Michel JP, Bouras C, Giannakopoulos P. 2004. Cortical microinfarcts and demyelination significantly affect cognition in brain aging. *Stroke* 35: 410–414.
- Majewska A, Yiu G, Yuste R. 2000. A custom-made two-photon microscope and deconvolution system. *Pflügers Arch* 441: 398–408.
- Misgeld T, Kerschensteiner M. 2006. In vivo imaging of the diseased nervous system. *Nat Rev Neurosci* 7: 449–463.
- Nguyen Q-T, Tsai PS, Kleinfeld D. 2006. MPSScope: A versatile software suite for multiphoton microscopy. *J Neurosci Methods* 156: 351–359.
- Nguyen J, Nishimura N, Iadecola C, Schaffer CB. 2007. Single venule occlusions induced by photodisruption using femtosecond laser pulses cause decreased blood flow in rat cortex. In *Society for neuroscience*. Society for Neuroscience, San Diego.
- Nguyen Q-T, Dolnick EM, Driscoll J, Kleinfeld D. 2009. MPSScope 2.0: A computer system for two-photon laser scanning microscopy with concurrent plasma-mediated ablation and electrophysiology. In *Methods for in vivo optical imaging*, 2nd ed. (ed. Frostig RD), pp. 117–142. CRC Press, Boca Raton, FL.
- Nishimura N, Schaffer CB, Friedman B, Tsai PS, Lyden PD, Kleinfeld D. 2006. Targeted insult to individual subsurface cortical blood vessels using ultrashort laser pulses: Three models of stroke. *Nat Methods* 3: 99–108.



A.Y. Shih et al.

- Nishimura N, Schaffer CB, Friedman B, Lyden PD, Kleinfeld D. 2007. Penetrating arterioles are a bottleneck in the perfusion of neocortex. *Proc Natl Acad Sci* **104**: 365–370.
- Nishimura N, Rosidi NL, Iadecola C, Schaffer CB. 2010. Limitations of collateral flow after occlusion of a single cortical penetrating arteriole. *J Cereb Blood Flow Metab* **30**: 1914–1927.
- Schaffer CB, Brodeur A, Mazur E. 2001. Laser-induced breakdown and damage in bulk transparent materials induced by tightly-focused femtosecond laser pulses. *Meas Sci Technol* **12**: 1784–1794.
- Schaffer CB, Friedman B, Nishimura N, Schroeder LF, Tsai PS, Ebner FF, Lyden PD, Kleinfeld D. 2006. Two-photon imaging of cortical surface microvessels reveals a robust redistribution in blood flow after vascular occlusion. *PLoS Biol* **4**: e22. doi: 10.1371/journal.pbio.0040022.
- Shih AY, Friedman B, Drew PJ, Tsai PS, Lyden PD, Kleinfeld D. 2009. Active dilation of penetrating arterioles restores red blood cell flux to penumbral neocortex after focal stroke. *J Cereb Blood Flow Metab* **29**: 738–751.
- Sigler A, Goroshkov A, Murphy TH. 2008. Hardware and methodology for targeting single brain arterioles for photothrombotic stroke on an upright microscope. *J Neurosci Methods* **170**: 35–44.
- Stosiek C, Garaschuk O, Holthoff K, Konnerth A. 2003. In vivo two-photon calcium imaging of neuronal networks. *Proc Natl Acad Sci* **100**: 7319–7324.
- Suter OC, Sunthorn T, Kraftsik R, Straubel J, Darekar P, Khalili K, Miklossy J. 2002. Cerebral hypoperfusion generates cortical watershed microinfarcts in Alzheimer disease. *Stroke* **33**: 1986–1992.
- Tsai PS, Kleinfeld D. 2009. In vivo two-photon laser scanning microscopy with concurrent plasma-mediated ablation: Principles and hardware realization. In *Methods for in vivo optical imaging*, 2nd ed. (ed. Frostig RD), pp. 59–115. CRC Press, Boca Raton, FL.
- Tsai PS, Friedman B, Squier JA, Kleinfeld D. 2004. Ultrashort pulsed laser light: A cool tool for ultraprecise cutting of tissue and cells. *Optics & Photonic News* **14**: 24–29.
- Tsai PS, Friedman B, Schaffer CB, Squier JA, Kleinfeld D. 2005. All-optical, in situ histology of neuronal tissue with femtosecond laser pulses. In *Imaging in neuroscience and development: A laboratory manual* (ed. Yuste R, Konnerth A), pp. 815–826. Cold Spring Harbor Laboratory Press, Cold Spring Harbor, NY.
- Tsai PS, Blinder P, Migliori BJ, Neev J, Jin Y, Squier JA, Kleinfeld D. 2009. Plasma-mediated ablation: An optical tool for submicrometer surgery on neuronal and vascular systems. *Curr Opin Biotechnol* **20**: 90–99.
- Watson BD, Dietrich WD, Busto R, Wachtel MS, Ginsberg MD. 1985. Induction of reproducible brain infarction by photochemically initiated thrombosis. *Ann Neurol* **17**: 497–504.
- Watson BD, Prado R, Veloso A, Brunschwig JP, Dietrich WD. 2002. Cerebral blood flow restoration and reperfusion injury after ultraviolet laser-facilitated middle cerebral artery recanalization in rat thrombotic stroke. *Stroke* **33**: 428–434.
- Xu HT, Pan F, Yang G, Gan WB. 2007. Choice of cranial window type for in vivo imaging affects dendritic spine turnover in the cortex. *Nat Neurosci* **10**: 549–551.
- Zhang S, Boyd J, Delaney KR, Murphy TH. 2005. Rapid reversible changes in dendritic spine structure in vivo gated by the degree of ischemia. *J Neurosci* **25**: 5333–5338.